9774–9787 *Nucleic Acids Research, 2012, Vol. 40, No. 19* *Published online 27 July 2012*
doi:10.1093/nar/gks704

The role of Ca^{2+} in the activity of *Mycobacterium tuberculosis* DNA gyrase

Shantanu Karkare[1], Faridoon Yousafzai[2], Lesley A. Mitchenall[1] and Anthony Maxwell[1,*]

[1]Departments of Biological Chemistry and [2]Computational and Systems Biology, John Innes Centre, Norwich Research Park, Norwich NR4 7UH, UK

Received May 10, 2012; Revised and Accepted June 27, 2012

ABSTRACT

DNA gyrase is the only type II topoisomerase in *Mycobacterium tuberculosis* and needs to catalyse DNA supercoiling, relaxation and decatenation reactions in order to fulfil the functions normally carried out by gyrase and DNA topoisomerase IV in other bacteria. We have obtained evidence for the existence of a Ca^{2+}-binding site in the GyrA subunit of *M. tuberculosis* gyrase. Ca^{2+} cannot support topoisomerase reactions in the absence of Mg^{2+}, but partial removal of Ca^{2+} from GyrA by dialysis against EGTA leads to a modest loss in relaxation activity that can be restored by adding back Ca^{2+}. More extensive removal of Ca^{2+} by denaturation of GyrA and dialysis against EGTA results in an enzyme with greatly reduced enzyme activities. Mutation of the proposed Ca^{2+}-binding residues also leads to loss of activity. We propose that Ca^{2+} has a regulatory role in *M. tuberculosis* gyrase and suggest a model for the modulation of gyrase activity by Ca^{2+} binding.

INTRODUCTION

Tuberculosis (TB) is an infectious disease caused by the Gram-positive Actinobacteria *Mycobacterium tuberculosis*. According to the WHO report, Global Tuberculosis Control, published in 2011 (http://www.who.int/tb/publications/global_report/en/), approximately 8.8 million cases of TB occurred in 2010 and approximately 1.45 million deaths, making it the world's most deadly infectious bacterial disease; it is estimated that approximately 2 billion people are infected with TB worldwide. Two factors, persistence and resistance, make treatment of TB problematic (1,2). Persistence refers to bacteria that evade antibiotic treatment despite not being genetically resistant, for example by being in an environment that avoids drug exposure. This leads to the necessity for long courses of drug treatment. Resistance is due to genetic mutations and is manifested by MDR (multidrug-resistant) and XDR (extensively drug-resistant) TB strains. MDR strains are resistant to first-line drugs, isoniazid and rifampicin, while XDR strains are also resistant to fluoroquinolones and at least one injectable antibiotic. The existence of such strains leads to the spectre of untreatable TB.

Although there are a number of drugs that can be used to treat TB, resistance and the difficulties involved in long-term treatment regimens mean that new agents are urgently needed (3,4). Moxifloxacin, a fluoroquinolone, has been successfully used against TB, particularly MDR strains (5), but the advent of XDR-TB means that other agents need to be developed. Moxifloxacin targets DNA gyrase a DNA topoisomerase present in all bacteria.

DNA topoisomerases are enzymes responsible for maintaining and manipulating the topological state of DNA (6–8). These enzymes are required for vital processes such as DNA replication, transcription, recombination and chromatin remodelling; they are found in all organisms including eukaryotes (yeast, plants and animals), prokaryotes, viruses and archaea. Topoisomerases can be classified into two types, I and II, dependent on whether their reactions involve transient cleavage of one (I) or both (II) strands of DNA. Due to the important role played by topoisomerases in maintaining cell viability, they are attractive clinical targets for chemotherapeutics (9–11). In addition, their mode of action involves transient DNA cleavage, which, if interrupted, can result in protein-associated DNA breaks and consequent cell death; a number of topoisomerase-targeted drugs, including fluoroquinolones, act in this way (9–11).

The presence and essentiality of gyrase in all bacteria and its absence from most eukaryotes (exceptions include plants and plasmodia), makes it an ideal target for antibacterial agents (9). The enzyme consists of two subunits, GyrA and GyrB, which form an A_2B_2 complex in the

*To whom correspondence should be addressed. Tel: +44 1603 450771; Fax: +44 1603 450018; Email: tony.maxwell@jic.ac.uk
Present address:
Shantanu Karkare, Novartis Institutes for BioMedical Research, Novartis Campus, CH-4056 Basel, Switzerland.

active enzyme (12,13). Gyrase is a type II topoisomerase that is unique; it is the only enzyme that can introduce negative supercoils into DNA, in a reaction coupled to the hydrolysis of ATP; other type II enzymes can only catalyse DNA relaxation and decatenation (12,13). The supercoiling reaction involves the binding of gyrase to ~130 bp of DNA, which is wrapped around the protein complex. The enzyme cleaves the wrapped DNA (at the so-called 'gate' or 'G' segment) forming a protein-associated double-stranded break involving active-site tyrosines present in GyrA. Another part of the wrapped segment (the 'transported' or 'T' segment) is passed through this break which is then resealed. Catalytic supercoiling requires the hydrolysis of ATP, which occurs in the GyrB subunits (12,13).

Most bacteria contain a second type II topoisomerase in addition to gyrase, called topoisomerase (topo) IV, which is specialized for carrying out decatenation and relaxation of supercoiled DNA (14–16). Certain bacteria, including *M. tuberculosis* and *M. smegmatis,* lack topo IV (17–19). One consequence of this is that the activities normally carried out by topo IV have to be carried out by gyrase. It has been found that the gyrases from *M. tuberculosis* and *M. smegmatis* are efficient decatenases (20,21) compared with gyrases from other species such as *Escherichia coli*.

To develop *M. tuberculosis* gyrase as a target for therapy and to help in the development of new TB drugs, a better understanding of the enzyme is required. The enzyme has been expressed as separate subunits in *E. coli* (17) and its reactions have been studied (20). Although it shares many characteristics of its *E. coli* counterpart it has distinguishing properties such as enhanced relaxation and decatenation activities. Key DNA-binding residues, involved in DNA wrapping in the C-terminal domain (CTD) of *M. tuberculosis* GyrA have been established (22) and mechanistic studies have investigated the role of GyrB in DNA strand passage (23). Recently, the structures of various domains of *M. tuberculosis* gyrase have been determined by X-ray crystallography: the CTD of GyrB (24), the N-terminal domain (NTD) of GyrA (25,26) and the CTD of GyrA (27). This work enables a better understanding of structure/function relationships in *M. tuberculosis* gyrase that will advance its further exploitation as a TB target.

In this article, we have obtained evidence for the existence of a Ca^{2+}-binding site in *M. tuberculosis* gyrase GyrA and we suggest that Ca^{2+} could play a role in regulating the activities of this enzyme. Although the importance of Ca^{2+} as a regulator in eukaryotes is well-established, its role in prokaryotes is less clear (28). However, it has been implicated in a variety of processes including DNA replication and cell division (29,30); our results raise the possibility of a role for Ca^{2+} in regulating the activities of gyrase, a key enzyme in DNA replication.

MATERIALS AND METHODS

Bioinformatics and modelling

ClustalW (31) and MUSCLE (EMBL-EBI) (32,33) were used for multiple sequence alignment, PSIPRED (34) was used for protein secondary structure prediction and PROSITE was used for predicting structural and functional patterns (35). Phyre (36), BioInfoBank MetaServer (37) and Insight II (Accelrys) were used for molecular modelling studies.

Enzymes and DNA

Mycobacterium tuberculosis DNA gyrase subunits were purified as described previously (22) with modifications. The expression plasmids were transformed into *E. coli* BL21(DE3)pLysS and an overnight culture of the cells was used to inoculate 1 L L-Broth, containing 100 μg/ml ampicillin and 30 μg/ml chloramphenicol. The cells were grown at 37°C to an OD_{600} = 0.4–0.6 and protein expression was induced by the addition of isopropyl β-D-1-thiogalactopyranoside to a final concentration of 0.4 mM and the culture was left shaking for 4 h at 37°C. The cells were harvested by centrifugation and resuspended in binding buffer [20 mM Tris–HCl (pH 7.9), 500 mM NaCl and 5 mM imidazole]. The cells were lysed by French press and a complete EDTA-free protease inhibitor cocktail tablet (Roche) was added. The cell debris was removed by centrifugation and the supernatant was purified using a HisTrap HP IMAC 5 ml column (Amersham Bioscience, USA) equilibrated with binding buffer. The column was washed initially with 20 mM Tris–HCl (pH 7.9), 500 mM NaCl and 60 mM imidazole and the His-tagged protein was eluted with 20 mM Tris–HCl (pH 7.9), 500 mM NaCl, with an imidazole gradient from 60 to 500 mM. The peak fractions were pooled based on their purity, analysed using SDS–PAGE and then dialysed against 50 mM Tris–HCl (pH 7.9), 30% glycerol, 5 mM dithiothreitol; proteins were concentrated using Amicon Ultra-4 columns and then stored at −20°C. Where experiments involved EGTA dialysis, protein was dialysed into the same buffer containing 1 mM EGTA.

For protein refolding experiments, protein was first dialysed into 50 mM Tris–HCl (pH 7.5), 100 mM KCl, 2 mM DTT, 8 M guanidine hydrochloride, 1 mM EDTA) at 37°C for 3 h. Then the protein was dialysed into 50 mM Tris–HCl (pH 7.5), 100 mM KCl, 2 mM DTT, 8 M urea, 1 mM EDTA and 10% glycerol at 4°C overnight. The next day the protein sample was dialysed into 50 mM Tris–HCl (pH 7.5), 100 mM KCl, 2 mM DTT, 1 mM EDTA and 10% glycerol to remove the denaturing agents and for protein refolding. Where protein samples were refolded in the presence of EGTA, all three buffers had 1 mM EGTA added. This protocol is a modified version of the protein refolding protocol used for recombining DNA gyrase subunits for transactivation experiment (38).

Supercoiled and relaxed forms of plasmid pBR322, and kDNA were from Inspiralis (Norwich, UK).

Enzyme assays

A typical supercoiling assay (30 μl) contained a range of gyrase concentrations (0.006–0.3 μM) and 0.5 μg of relaxed pBR322 in 40 mM Tris–HCl (pH 7.9), 25 mM KCl, 4 mM DTT, 0.1 mg/ml tRNA, 100 mM potassium glutamate, 0.36 mg/ml BSA, 6 mM magnesium acetate,

2 mM spermidine and 1 mM ATP. Reactions were incubated at 37°C for 60 min. After the incubation, DNA was prepared for electrophoresis by addition of an equal volume of chloroform:isoamylalcohol (24:1), brief vortexing, centrifugation and addition of 30 µl STEB [40% sucrose, 100 mM Tris–HCl (pH 8.0), 100 mM EDTA and 0.5 µg/ml bromophenol blue]. The products were analysed by electrophoresis on 1% agarose gels at 1 V/cm overnight and stained with ethidium bromide.

DNA relaxation assays were performed in a similar way, except ATP and spermidine were omitted and the substrate was supercoiled pBR322.

A typical decatenation assay (30 µl) containing a range of gyrase concentrations and 200 ng kDNA in 40 mM Tris–HCl (pH 7.9), 25 mM KCl, 4 mM DTT, 100 mM potassium glutamate, 0.36 mg/ml BSA, 6 mM magnesium acetate and 1 mM ATP. Reactions were incubated at 37°C for 60 min, and the DNA was analysed as described above.

For DNA wrapping experiments, the DNA relaxation assay was scaled up to 60 µl. After incubation at 37°C for 60 min, the reaction was divided into two; one half of the reaction was stopped with 15 µl STEB and the other half was incubated with 2 µl of wheat germ topo I (Promega: 2–10 U/µl) at 37°C for 30 min. The reaction was stopped with 3 µl 2% SDS, 0.2 µl proteinase K (20 mg/ml) and 15 µl STEB. The DNA was analysed as described above.

Site-directed mutants

Site-directed mutants were generated in pET20-gyrA using the Stratagene QuickChange® Lightning kit. Primers: GyrA-D504A (forward primer 5′-GGC CGA CGG AGC CGT CAG CGA C, reverse primer 5′-CGT CGC TGA CGG CTC CGT CGG CC); GyrA-E514A (forward primer 5′-TTG ATC GCC CGC GCG GAC GTC GTT GTC, reverse primer 5′-GAC AAC GAC GTC CGC GCG GGC GAT CAA); GyrA-E508A, D509A (forward primer 5′-GAC GTC AGC GAC GCG GCT TTG ATC GCC CGC, reverse primer 5′-GCG GGC GAT CAA AGC CGC GTC GCT GAC GTC).

Limited Proteolysis

Six micromolars of GyrA was incubated with 3 mM $CaCl_2$ at 25°C for 1 h; trypsin (1.8 µg/ml) was added and the incubation continued at 37°C in a total reaction mixture of 55 µl. Five microlitres of aliquots were collected at different times and the digestion was stopped by boiling the samples in 0.125 M Tris–HCl (pH 6.8), 4% SDS, 20% glycerol, 10% β-mercaptoethanol and 0.002% bromophenol blue. Samples were run on 12% SDS–PAGE gels.

To sequence protein products, 100–200 pmol of each protein sample was run in triplicate on a NuPAGE 10% Bis–Tris gels (Invitrogen) and then blotted onto a PVDF membrane using 10 mM CAPS (pH 11.0) with or without the inclusion of 10% methanol. For electroblotting, PVDF membranes were prepared by immersion in HPLC grade methanol for 20 s followed by equilibration in transfer buffer for 10 min. A gel/PVDF/blotting paper sandwich was prepared and a semi-dry blot performed at 1–3 mA/cm^2 for 45 min–1.5 h. After blotting, the PVDF membrane was immediately washed with water twice with 10 min shaking. The membrane was stained with 0.1% Coomassie Blue R250 in 50% methanol for 5 min and destained with several changes, 2–5 min each of 30–50% methanol. Finally, the membrane was washed in water and air-dryed and stored at −20°C. Edman sequencing was carried out by Dr Weldon,M.A. at Protein and Nucleic Acid Chemistry (PNAC) facility, Department of Biochemistry, Cambridge, UK.

ICP-AES

ICP-AES (inductively coupled plasma atomic emission spectroscopy) was used to determine the concentration of divalent ions in protein samples. Samples were analysed on Varian Vista Pro ICP using a spectral range of 315–317 nm, 15.0 l/min plasma flow, 1.05 l/min auxiliary flow and nebulizer flow, and a reading time of 5 s with six replicates.

RESULTS

Bioinformatics and modelling suggest a putative Ca^{2+}-binding site in *M. tuberculosis* GyrA

The DNA gyrase A protein has long been known to consist of two domains: an NTD of ∼60 kDa and a CTD of ∼30 kDa (Figure 1A) (39,40). The NTD is involved in binding DNA and contains some of the residues involved in DNA cleavage including the active-site tyrosine (12,13). The CTD is involved in DNA wrapping and is essential for DNA supercoiling (41,42). It is thought that there is a linker region between these domains that may be flexible in nature and involved in positioning the CTDs relative to the NTDs during the supercoiling cycle (43,44). However the structure of this linker (∼15 amino acids in *M. tuberculosis*) in GyrA is currently not known, although the structure of the comparable stretch of protein in *E. coli* ParC is (45), which in this case is a ∼20 amino acid linker with a well-ordered structure.

Multiple sequence alignment and bioinformatic analyses suggest that there may be a potential Ca^{2+}-binding motif in the linker regions between the GyrA NTD and CTD of *M. tuberculosis* and other bacterial species (Figure 1B): 504-DVSDEDLIAREDV-516 is a potential EF-hand Ca^{2+}-binding motif (46,47). Previous work has also suggested that EF-hand Ca^{2+}-binding motifs may be present in GyrA from mycobacteria and other species (30,46). The EF-hand proteins have a characteristic helix–loop–helix Ca^{2+}-binding motif and they constitute one of the largest protein families involved in numerous biological processes; there are >66 subfamilies (47–49). EF-hands are divided into two major groups, the canonical EF-hand (calmodulin and prokaryotic calerythrin) and the pseudo EF-hands, exclusively found in the N-termini of S100 and S100-like proteins (50). The majority of EF-hand motifs are paired; proteins with odd numbers of EF-hands are coupled through homo- or hetero-dimerisation.

The predicted Ca^{2+}-binding site in *M. tuberculosis* DNA gyrase does not follow the canonical EF-hand

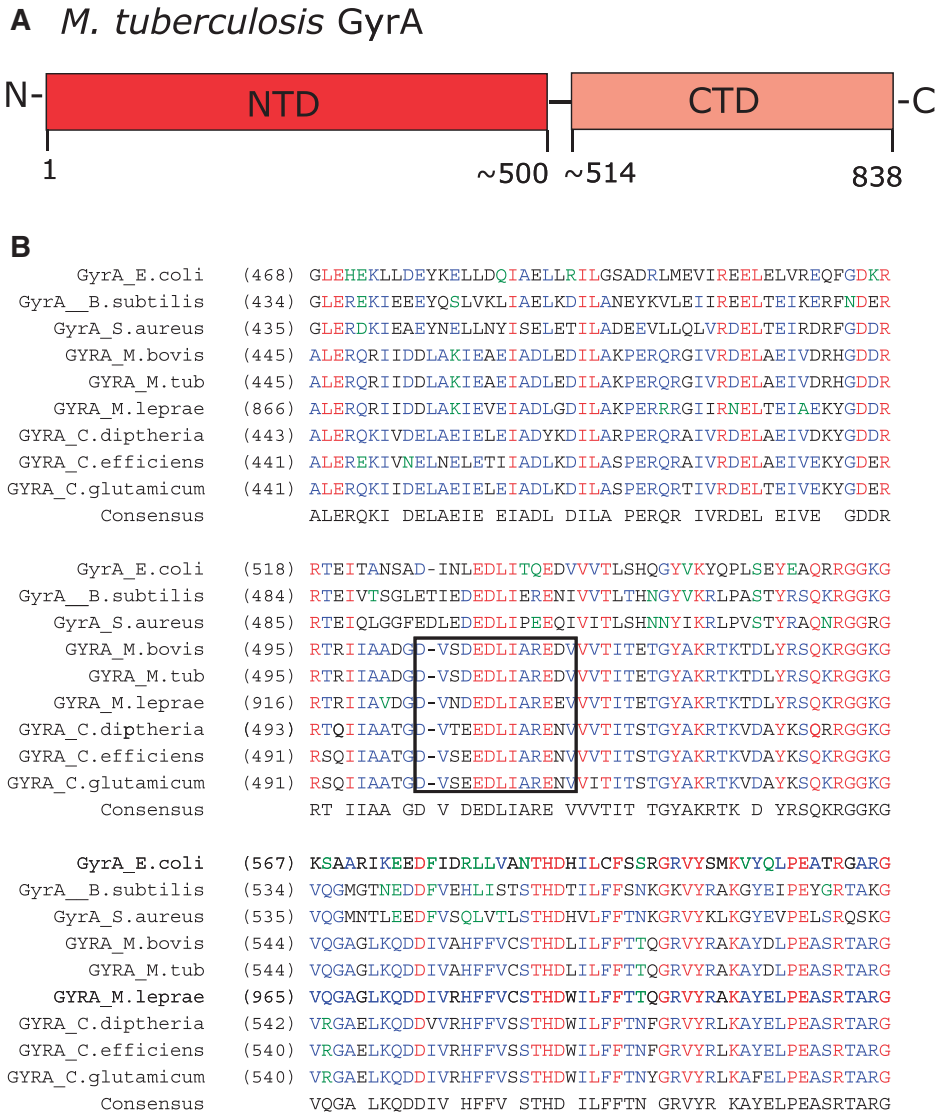

Figure 1. *Mycobacterium tuberculosis* GyrA. (**A**) Domain structure of GyrA showing the NTDs and the CTDs, and indicating the approximate boundaries of the linker region. (**B**) Alignment of GyrA sequences; the boxed region indicates the predicted Ca^{2+}-binding motif. E., *Escherichia*; B., *Bacillus*; S., *Staphylococcus*; M., *Mycobacterium*; C. *Corynebacterium*.

helix–loop–helix pattern; there are several examples of proteins in prokaryotes that do not follow the canonical definition of EF-hand Ca^{2+}-binding sites, such as the periplasmic glucose/galactose receptor [*Salmonella typhimurium*; Protein Data Bank (PDB) code: 1gcg; (51)] and alginate-binding protein [*Sphingomonas* sp. A1; PDB code: 1kwh; (52)].

Although crystal structures for the NTD of GyrA of *M. tuberculosis* GyrA [3ilw, 3ifz (25,26)] have been solved, these structures lack the putative Ca^{2+}-binding site and there is no crystal structure for the complete *M. tuberculosis* GyrA. Therefore we constructed a homology model. Two templates, psychrophilic metalloprotease from *Pseudoalteromonas* [PDB: 1h71 (53)] and *Staphylococcus aureus* metalloproteinase [PDB: 1bqb (54)] were identified for modelling the Ca^{2+}-binding site, which generated two models referred to as MtGyrA-1H71 and MtGyrA-1BQB (Figure 2). In MtGyrA-1H71, only one Ca^{2+} is coordinated to six residues: D504, S506, E508, L510, A512 and E514 (Figure 2A), whereas in MtGyrA-1BQB, two Ca^{2+} ions are coordinated by three water molecules in addition to S506, E508, D509, I511, E514 and E586 (Figure 2B). Mutation studies (see below) were designed to evaluate these models.

Ca^{2+} supports DNA supercoiling and promotes DNA cleavage with *E. coli* gyrase but only limited activity with *M. tuberculosis* gyrase

Previous work has shown that *E. coli* gyrase can supercoil DNA when Ca^{2+} is substituted for Mg^{2+}, and that Ca^{2+} also stabilizes the DNA cleavage complex (39,55) (Figure 3A). Despite the presence of a putative Ca^{2+}-binding site in *M. tuberculosis* GyrA, we found that the enzyme had very little supercoiling activity when Ca^{2+} is

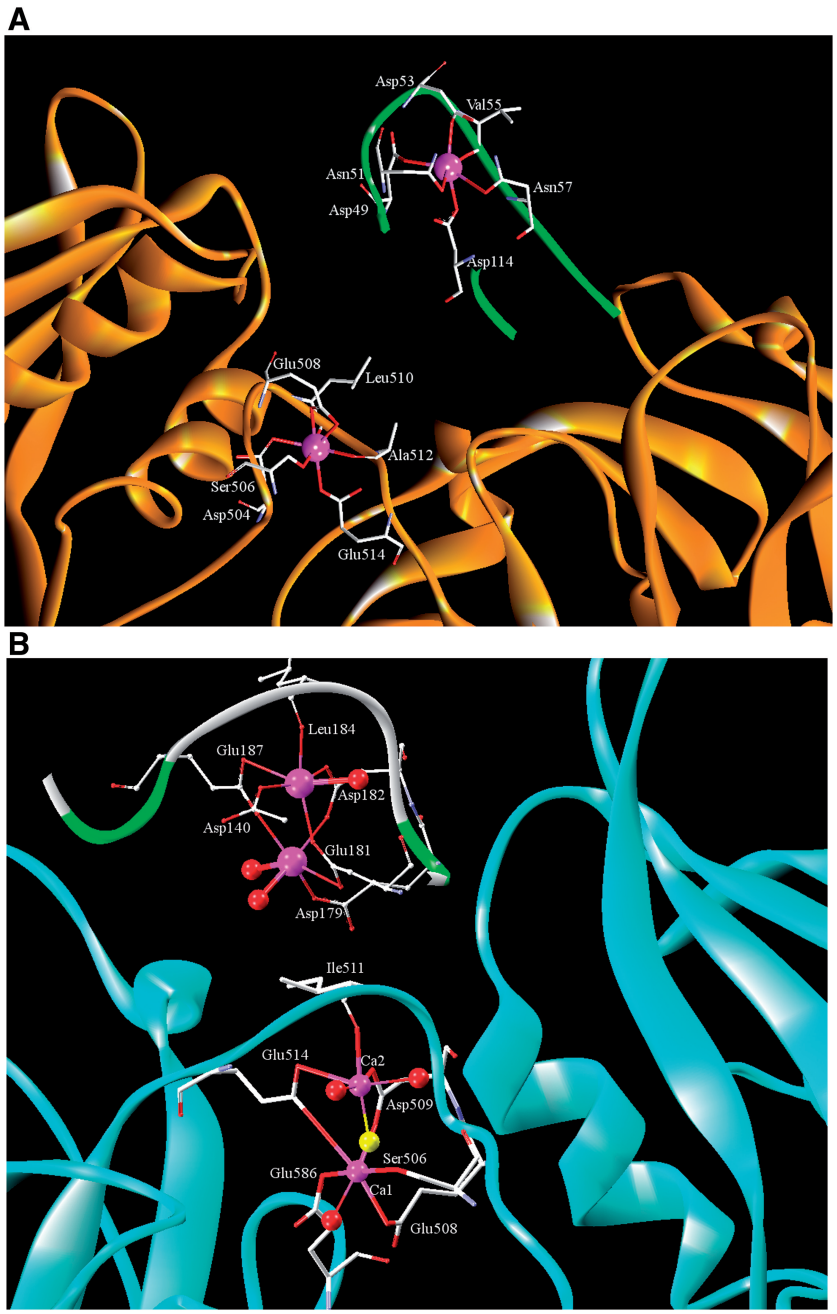

Figure 2. Models of the *M. tuberculosis* GyrA Ca^{2+}-binding site. (**A**) Homology model of the *M. tuberculosis* GyrA Ca^{2+}-binding site (MtGyrA-1H71) based on the psychrophilic metalloprotease from Pseudomonas sp. (PDB code: 1H71). The Ca^{2+}-binding site in 1H71 is shown above the GyrA Ca^{2+}-binding site for comparison. (**B**) Homology model of *M. tuberculosis* GyrA Ca^{2+}-binding site (MtGyrA-1BQB) based on *S. aureus* metalloproteinase (PDB code: 1BQB). One water molecule coordinates $Ca^{2+}1$ and three water molecules coordinate $Ca^{2+}2$, as represented by yellow and red balls. The Ca^{2+}-binding site in 1BQB is shown above the GyrA Ca^{2+}-binding site for comparison.

substituted for Mg^{2+}, consistent with a previous report (20) (Figure 3B), and that Ca^{2+} was unable to stabilize the gyrase cleavage complex (data not shown). To attempt to link this loss of activity to a specific subunit, we made hetero-tetramers between the GyrA and GyrB subunits of *E. coli* and *M. tuberculosis* gyrases. When *M. tuberculosis* GyrA was mixed with *E. coli* GyrB to create the hybrid enzyme, MtA_2EcB_2, it exhibited supercoiling activity in the presence of 6 mM Mg^{2+}; the converse hybrid: EcA_2MtB_2, exhibited very little activity in the presence of Mg^{2+} (Figure 3C). Neither hybrid enzyme showed significant activity in the presence of Ca^{2+} (Supplementary Figure S1). The data suggest that Mg^{2+} is required for DNA supercoiling by *M. tuberculosis* gyrase and that Ca^{2+} is unable to efficiently support this reaction. Previous work has shown that Ca^{2+} is also unable to support DNA relaxation by *M. tuberculosis* gyrase (20). It is possible that the enzyme has specialized roles for the different divalent ions, i.e. Ca^{2+} may have a regulatory role.

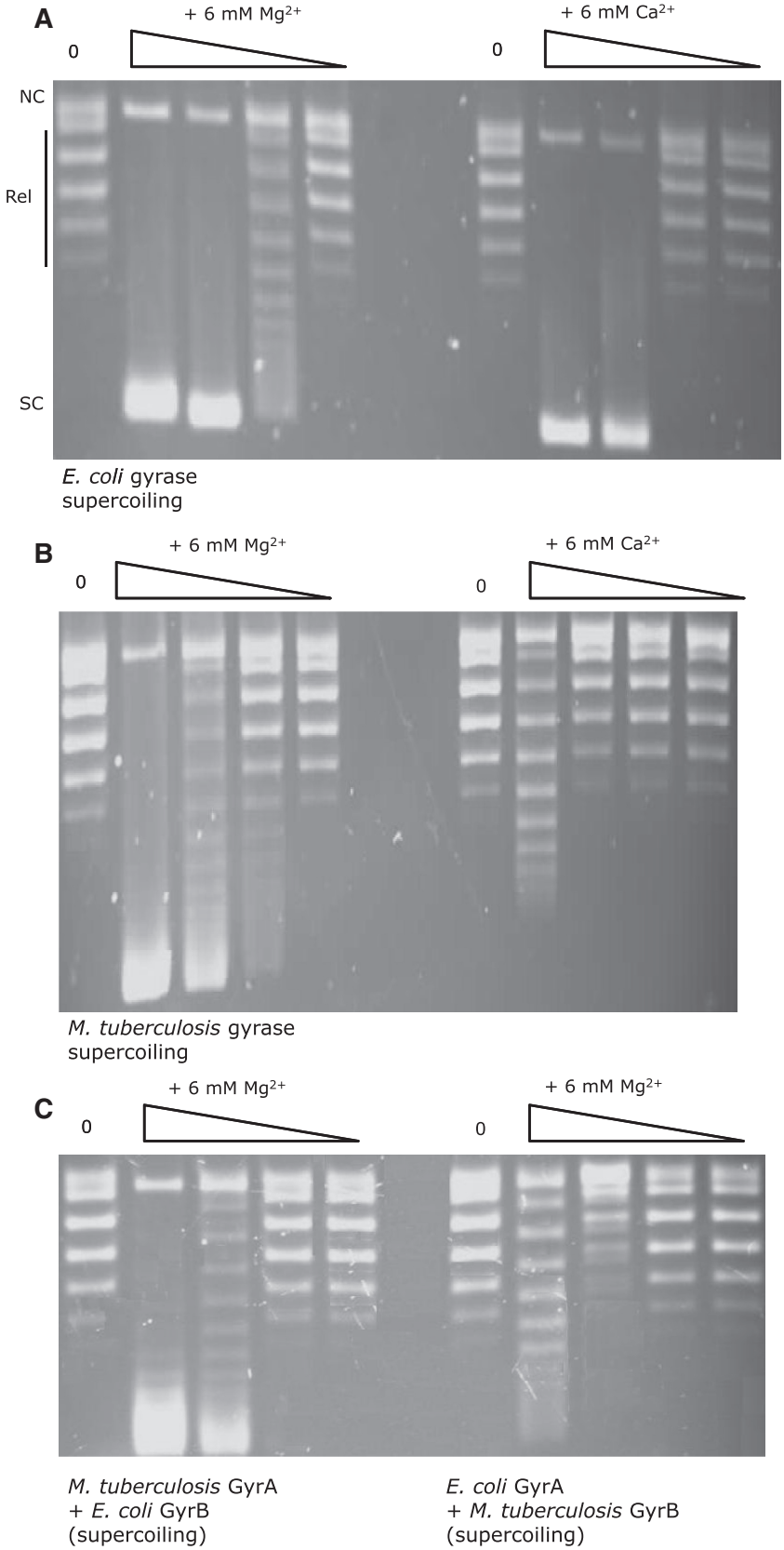

Figure 3. Ca^{2+}can support supercoiling by *E. coli* gyrase but not *M. tuberculosis* gyrase. Supercoiling assays with *E. coli* (**A**) and *M. tuberculosis* gyrases (**B**), and hybrid enzymes (**C**) in the presence of 6 mM Mg^{2+} and Ca^{2+}. Enzyme concentrations ([E]) were: 0.006, 0.018, 0.054 and 0.16 μM; 0: no enzyme; NC: nicked-circular DNA; Rel: relaxed topoisomers; SC: supercoiled DNA.

Ca^{2+} stimulates Mg^{2+}-dependent topoisomerase activities of *M. tuberculosis* gyrase

As Ca^{2+} could not substitute for Mg^{2+} to support supercoiling by *M. tuberculosis* gyrase (Figure 3), we investigated other possible roles for Ca^{2+} in *M. tuberculosis* gyrase reactions. To do this, we attempted to remove any bound Ca^{2+} from the enzyme. Initially we dialysed the *M. tuberculosis* gyrase subunits, separately, against EGTA. We found that there was no effect on the supercoiling or decatenation reactions of *M. tuberculosis* gyrase; dialysis of GyrB versus EGTA had no influence on any reactions (Supplementary Figure S2). However, we found that *M. tuberculosis* GyrA that had been dialysed against EGTA consistently showed a 2- to 3-fold loss in relaxation activity (Figure 4A and C); moreover, this activity could be restored by the addition of 1 mM $CaCl_2$ (Figure 4C and D). Adding 1 mM Ca^{2+} to reactions containing 6 mM Mg^{2+} had no apparent effect on activity (Figure 4B). This effect of removing Ca^{2+} from the enzyme was also revealed from a relaxation time course (Figure 4E), which again suggested a ~3-fold loss in activity. (Note that the apparent increase in supercoiling observed at later times in the left panel is due to DNA wrapping by gyrase leading to a low level of positive supercoiling in these lanes.)

To further investigate this phenomenon, *M. tuberculosis* GyrA was denatured prior to dialysis and refolded either in the absence or presence of EGTA (to remove any tightly bound Ca^{2+}). In order to avoid Ca^{2+} contamination, *M. tuberculosis* GyrB was also dialysed in the presence of EGTA. GyrA that had been denatured and refolded showed no significant loss in supercoiling or relaxation activities (Figures 5A and C). By contrast, GyrA that had been denatured and refolded in the presence of EGTA showed reduced supercoiling activity (Figure 5B) and complete loss of relaxation activity (Figure 5D). Enzyme treated this way also showed complete loss of decatenation activity (data not shown). Taken together these data suggest that when Ca^{2+} is removed from *M. tuberculosis* gyrase there is a loss in enzyme activity. Partial removal, by dialysis of the enzyme against EGTA, results in no change in supercoiling activity but a modest loss in relaxation activity that can be restored by re-addition of Ca^{2+}. More aggressive removal of Ca^{2+}, by denaturation and refolding by dialysis in the presence of EGTA leads to significant loss in supercoiling activity and complete loss of relaxation activity (Table 1). These data provide evidence for a differential effect of Ca^{2+} on the supercoiling and relaxation reactions (see 'Discussion' section).

Site-directed mutagenesis of putative Ca^{2+}-binding residues in *M. tuberculosis* gyrase leads to loss of supercoiling activity associated with loss of DNA wrapping

Based on the models of the putative Ca^{2+}-binding sites in *M. tuberculosis* GyrA described above (Figure 2), GyrA proteins containing double (E508A and D509A) and quadruple (D504A, E508A, D509A and E514A) amino acid substitutions were created by site-directed mutagenesis. Some of these residues are involved in both the MtGyrA-1H71 and MtGyrA-1BQB models (E508 and E514); D509 is involved in coordinating Ca^{2+} only in MtGyrA-1BQB and D504 is involved in coordinating Ca^{2+} only in MtGyrA-1H71.

We found no significant effect of the double mutation (E508A and D509A) on the supercoiling activity of *M. tuberculosis* gyrase, although the supercoiling activity may be slightly reduced (Figure 6B). The quadruple mutant (D504A, E508A, D509A and E514A), seems to only be able to reach partial supercoiling. [This effect was even more marked when the supercoiling assay was performed in buffer having magnesium chloride rather than magnesium acetate and without potassium glutamate (data not shown).] The quadruple mutant displays normal relaxation and decatenation activity. In previous work it was found that the GyrA mutation E514A had a slight effect on relaxation activity but no effect on decatenation (22). Interestingly we noted that while the ATP-dependent decatenation activity of the quadruple mutant was comparable to wild-type, the mini-circle products were predominantly relaxed rather than supercoiled, consistent with the inability of the mutant to supercoil DNA (Supplementary Figure S3). These data would suggest that the loss of supercoiling activity is not due to protein inactivation by mis-folding. Additionally, CD analysis showed no evidence of mis-folding for the quadruple mutant, or following treatment with EGTA (Supplementary Figure S4).

The altered supercoiling activity of the quadruple mutant and normal decatenation and relaxation activities suggests that the mutations may have affected DNA wrapping. This was demonstrated by performing topo I relaxation of the gyrase-DNA complex. Previous work has shown that the incubation of gyrase and DNA and subsequent addition of topo I leads to the generation of positively supercoiled DNA (13,56), consistent with the wrapping of DNA around the enzyme. As shown in Figure 7, positively supercoiled DNA is produced in the case of wild-type GyrA after topo I treatment, which is not observed in the case of the quadruple mutant, indicating that the mutations affect DNA wrapping. This effect on wrapping could be attributable to the reduced ability of the mutant GyrA subunit to bind Ca^{2+}, suggesting that Ca^{2+} may be important for enabling the wrapping of DNA prior to supercoiling (see 'Discussion' section).

Limited Proteolysis

In order to explore potential structural changes in the Mt GyrA protein due to the presence or absence of Ca^{2+}, limited proteolysis was carried out. As shown in Figure 8, there are differences between the trypsin digestion profile of GyrA in the presence and absence of 3 mM $CaCl_2$. In the presence of Ca^{2+}, GyrA appears to be more susceptible to trypsin than in its absence. (For comparison, the presence of Ca^{2+} had no effect on tryptic digests of GyrB; Supplementary Figure S5.) The main digestion product in the presence of Ca^{2+} was a ~54 kDa band (*2*); in the absence of Ca^{2+} a ~47 kDa band (*3*) was more

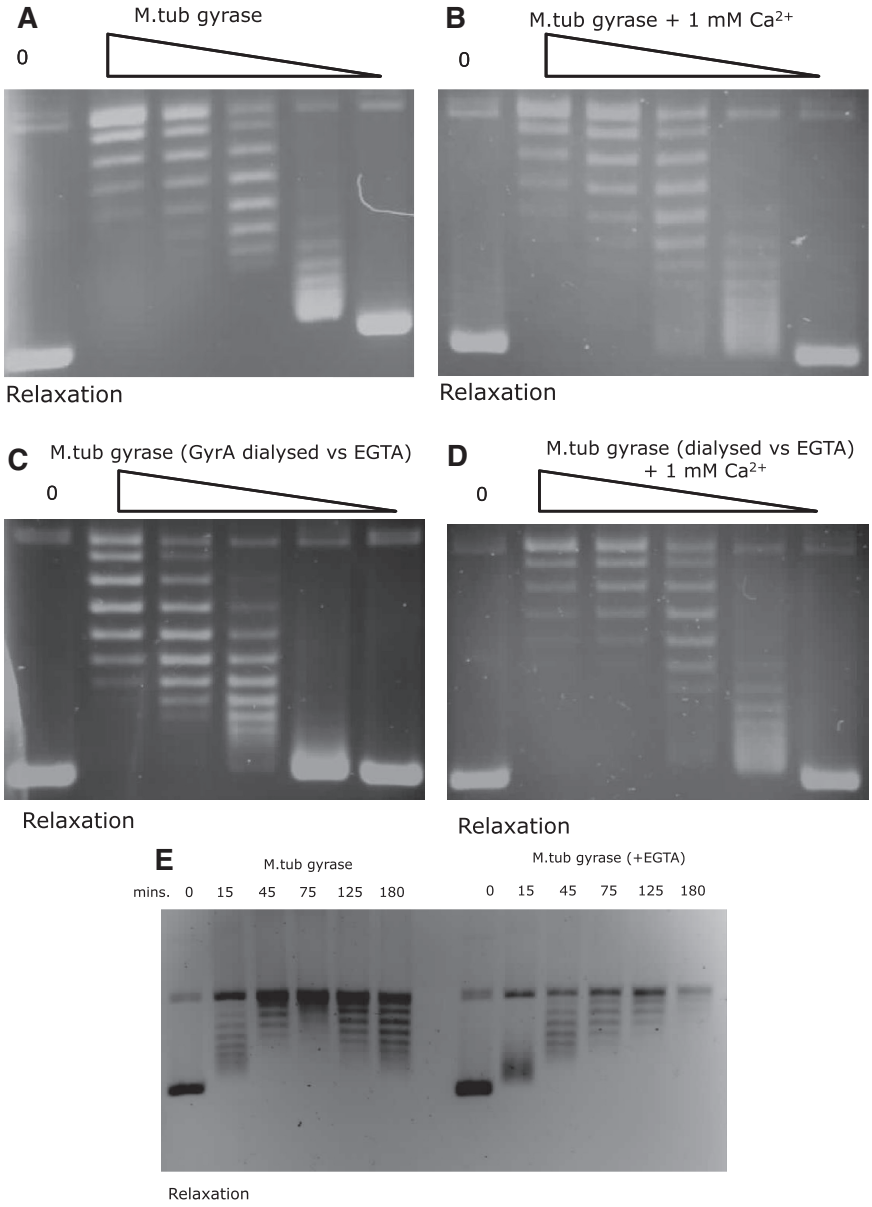

Figure 4. DNA relaxation by *M. tuberculosis* gyrase is stimulated by Ca^{2+}. DNA relaxation by *M. tuberculosis* gyrase in the absence (**A** and **C**) and presence (**B** and **D**) of 1 mM Ca^{2+}. In (C) and (D) the GyrA had been extensively dialysed against EGTA. Enzyme concentrations ([E]) were: 0.01, 0.04, 0.07, 0.10 and 0.13 μM; 0: no enzyme. (**E**) Time-course experiment to demonstrate the difference in the relaxation activity of gyrase with GyrA dialysed in the absence (left) and presence (right) of EGTA.

prominent. Edman sequencing of these bands showed that Band *2* was produced by cleavage after R26 (S27-G503) and Band *3* by cleavage after R128 (Y129-K542). The Ca^{2+}-binding site in *M. tuberculosis* GyrA is proposed to be V505–V515; it is interesting to note that Band *2* terminates approximately at the beginning of the proposed Ca^{2+}-binding site, and that Band *3* contains this sequence. It is possible that Ca^{2+} may stabilize a conformation of GyrA that lead to alterations in trypsin sensitivity.

Metal analysis shows the presence of two Ca^{2+} ions per *M. tuberculosis* GyrA monomer

ICP-MS (mass spectrometry) was used to measure the concentrations of Ca^{2+} in GyrA samples. We found ~50 μM Ca^{2+} associated with 20 μM of *M. tuberculosis* GyrA, suggesting an average of 2.5 Ca^{2+} ions per protein monomer. GyrA that had been denatured and refolded in the presence of EGTA showed ~30 μM Ca^{2+} with 20 μM of GyrA, 1.5 Ca on average per monomer, suggesting that one Ca^{2+} per monomer is removed by this procedure. These findings are potentially consistent with the MtGyrA-1BQB model (Figure 2), i.e. two Ca^{2+} ions per *M. tuberculosis* GyrA subunit or four Ca^{2+} ions per *M. tuberculosis* GyrA dimer.

Taken together these data suggest that there are Ca^{2+} ions tightly associated with *M. tuberculosis* GyrA (~two per monomer) and that these ions have a role in topoisomerase reactions. Partial removal of Ca^{2+} leads to some loss

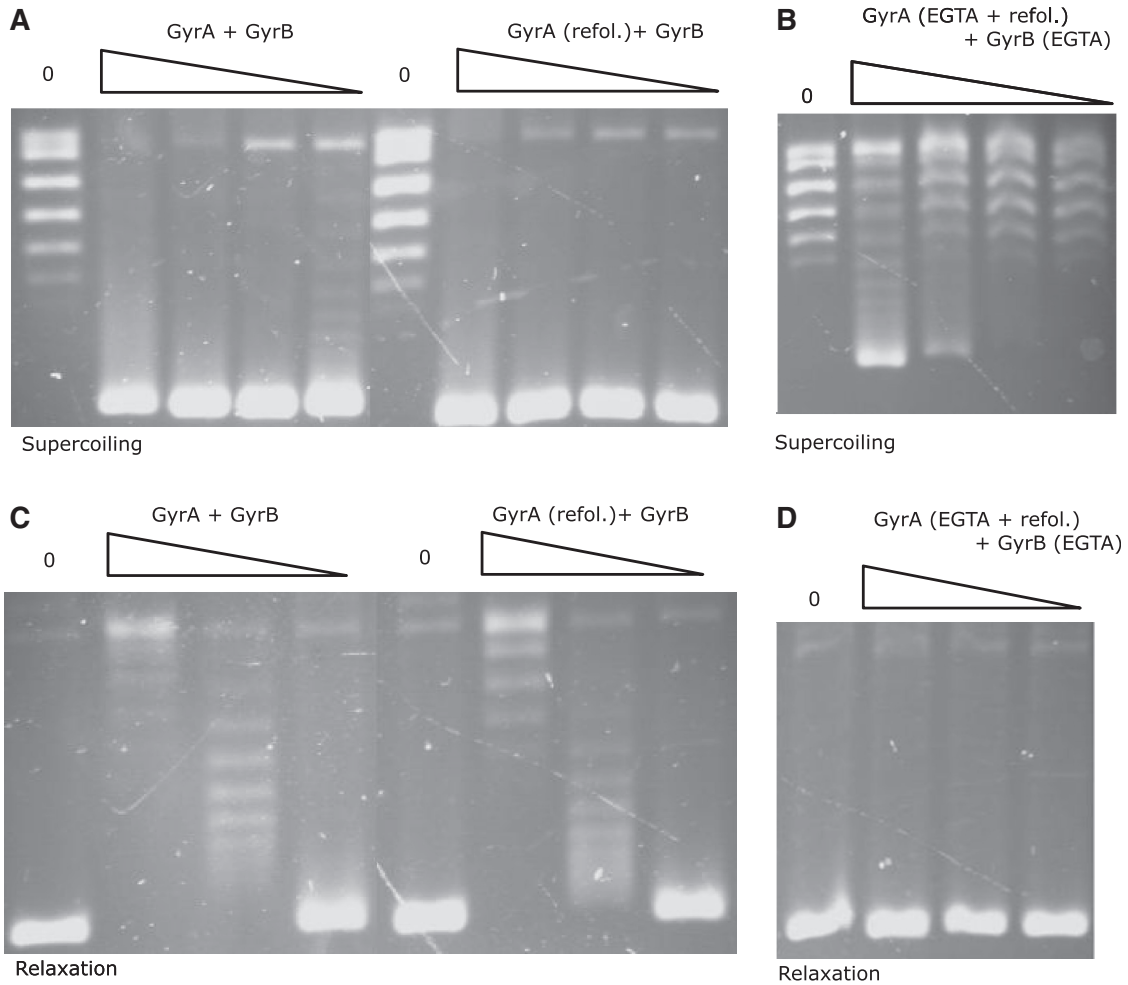

Figure 5. Effect of denaturation and dialysis against EGTA on supercoiling and relaxation by *M. tuberculosis* gyrase. Untreated GyrA and GyrB, or samples that had been denatured and refolded (refol.) in the absence or presence of EGTA, as indicated, were assayed for supercoiling (**A** and **B**) and relaxation (**C** and **D**). Enzyme concentrations ([E]) (A and B): 0.018, 0.05, 0.16 and 0.30 μM; (C and D): 0.03, 0.09 and 0.27 μM; 0: no enzyme.

of relaxation that can be restored by adding back Ca^{2+}; removal by denaturation/renaturation in the presence of EGTA leads to almost complete loss of activity.

DISCUSSION

Bioinformatic analysis suggested the presence of a Ca^{2+}-binding site in the GyrA subunit of *M. tuberculosis* DNA gyrase and also gyrases from other bacteria, e.g. *Corynebacterium* spp. (Figure 1); evidence for such a site has also been obtained previously (30,46). For example, a Ca^{2+}-binding site was predicted to be present in GyrA of *M. bovis* (46), which is a closely related species to *M. tuberculosis* and forms part of the *M. tuberculosis* complex (57). The predicted Ca^{2+}-binding sequence in *M. bovis* is also present in *M. tuberculosis*, '504-DVSDEDLIAREDV-516'. It is interesting to note that *Corynebacterium* spp, like *Mycobacterium* spp., also lack topo IV (58,59).

This proposed Ca^{2+}-binding site lies in the linker region between the NTDs and the CTDs of the protein. There is currently no structural information available for this region of GyrA, although a structure exists for the corresponding region of *E. coli* topo IV (45); however, there is no analogous sequence in the linker region of ParC, suggesting that topo IV does not contain a Ca^{2+}-binding site.

To explore the possibility of a Ca^{2+}-binding site in *M. tuberculosis* GyrA, two homology models were generated: MtGyrA-1H71 and MtGyrA-1BQB (Figure 2). The predicted Ca^{2+}-binding site in GyrA is an EF-hand-like binding site, but it does not follow the standard helix–loop–helix pattern, rather a loop–helix–loop–strand. Other examples of bacterial proteins that do not follow the standard helix–loop–helix pattern include the periplasmic galactose-binding protein from *S. typhimurium* (PDB code: 1gcg), which has a helix–loop–strand pattern (46,51). The Ca^{2+}-binding site seems to follow the loop and PS00018 patterns, which have been used for bioinformatics prediction of canonical EF-hand Ca^{2+}-binding sites (46).

Biochemical assays showed that Ca^{2+}could not be substituted for Mg^{2+} in *M. tuberculosis* gyrase supercoiling assays. However, we found that dialysis of

Table 1. Summary of the effect of EGTA dialysis and refolding on enzyme activity

Mycobacterium tuberculosis DNA gyrase		Supercoiling activity	Relaxation activity	Decatenation activity
GyrA	GyrB			
Untreated	Untreated	+++[a]	+++	+++
Refolded	Untreated	+++	+++	+++
Refolded + EGTA-dialysed	EGTA-dialysed	+	No activity	No activity

[a]Plus symbols represent ~3-fold difference in the enzyme activity.

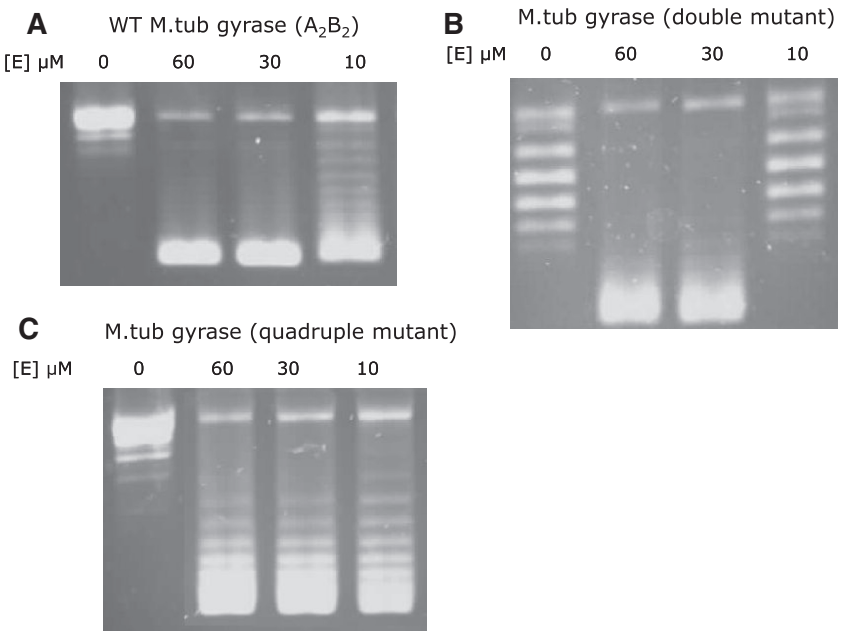

Figure 6. Mutations in the putative Ca^{2+}-binding site affect the supercoiling activity of *M. tuberculosis* gyrase. Effect of double ($GyrA^{E508A,D509A}$) and quadruple ($GyrA^{D504A,E508A,D509A,E514A}$) mutations on supercoiling activity. (**A**) Supercoiling activity of wild-type *M. tuberculosis* gyrase (A_2B_2). (**B**) Supercoiling activity of *M. tuberculosis* $GyrA^{(E508A,D509A)}{}_2B_2$. (**C**) Supercoiling activity of *M. tuberculosis* $GyrA^{(D504A,E508A,D509A,E514A)}{}_2B_2$.

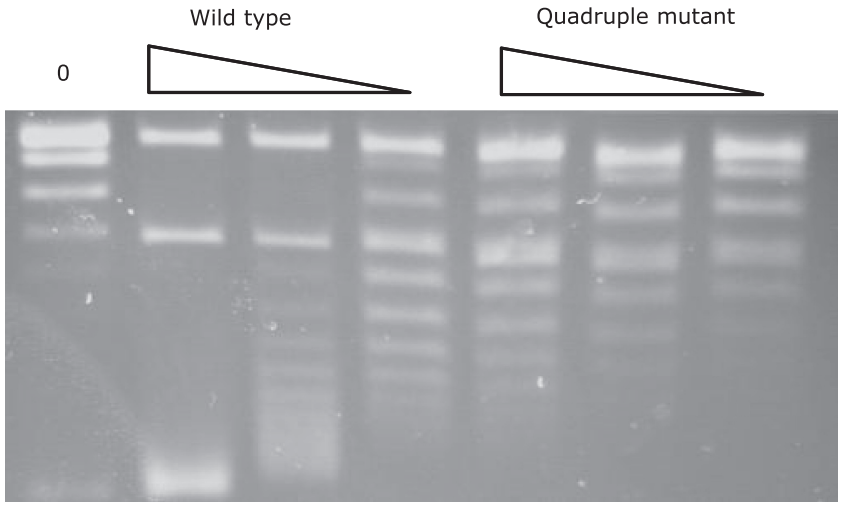

Figure 7. Wrapping experiment. Gyrase (wild-type or quadruple mutant; 0.13, 0.2 and 0.3 μM, as indicated) was incubated with supercoiled pBR322 DNA for 1 h at 37°C. Samples were then treated with wheat germ topoisomerase I for 30 mins at 37°C.

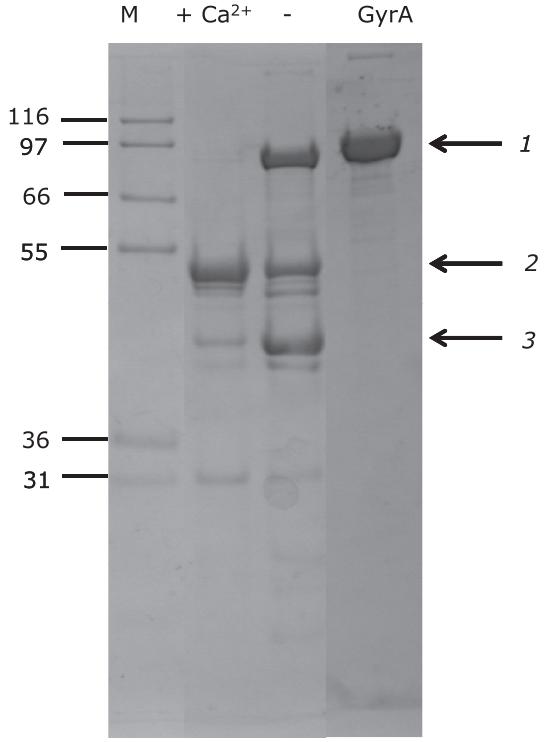

Figure 8. Tryptic digests of GyrA with and without Ca^{2+}. GyrA indicates untreated protein; minus symbol indicates tryptic digest in the absence of $CaCl_2$; +Ca indicates tryptic digest in the presence of 3 mM Ca^{2+}; M indicates molecular weight markers (116, 97, 66, 55, 36 and 31 kDa). Arrows indicate protein bands of interest: *1* = GyrA (97 kDa); *2* = ~54 kDa (S27-G503); *3* = ~47 kDa (Y129–K542).

M. tuberculosis gyrase versus EGTA had no apparent effect on supercoiling but led to a modest loss of relaxation activity that could be restored by re-addition of Ca^{2+}. More aggressive removal of Ca^{2+} involving denaturation and refolding in the presence of EGTA, led to some loss in supercoiling activity and disruption of relaxation and decatenation activities. This may support the presence of both loosely bound and tightly bound Ca^{2+} and might support a model with two Ca^{2+} ions per GyrA (MtGyrA-1BQB; Figure 2); ICP-AES analysis also favours at least two Ca^{2+} ions per GyrA.

Site-directed mutagenesis experiments in which key proposed Ca^{2+}-binding residues in GyrA were mutated showed no effects on relaxation and decatenation but marked effects on supercoiling. The effect on supercoiling appears to be correlated with an alteration of DNA wrapping. As we do not currently know the structure of the proposed Ca^{2+}-binding site in *M. tuberculosis* GyrA, it is not clear what effects these mutations might have on Ca^{2+} binding. Site-directed mutagenesis has been extensively used to probe Ca^{2+}-binding in proteins (47). Mutation of acidic residues in Ca^{2+}-binding sites can have a variety of effects depending on the position of the amino acid and nature of the mutation. For example, in calmodulin, Asp-to-Asn mutations led to increases or decreases in Ca^{2+} affinity and the cooperativity of binding, depending on their location (60). In other work a series of mutants in calmodulin were made to probe the relationship between Ca^{2+} affinity and the number of paired acidic residues (61), which showed a range of responses in terms of changes in Ca^{2+} affinity.

GyrA is known to consist of two domains that have distinct functions. The NTD contains the active-site tyrosine and is involved in the binding and cleavage of the bound G segment. The CTD is involved in DNA wrapping and presentation of the T segment to the G segment prior to strand passage (62). Structural work (44,45) suggests that the region between the NTD and the CTD comprises a flexible linker and that the CTD can adopt at least two positional states: an upper conformation, suitable for DNA wrapping (63), and a lower conformation that may represent a 'post-strand passage' or 'resting' state (43–45) (Figure 9). It is proposed that the enzyme can shuttle between these two states during T-segment passage through the enzyme during the supercoiling cycle (44,45). Recent single molecule fluorescence resonance energy transfer experiments with *Bacillus subtilis* gyrase support a model in which the GyrA CTDs are in a lower configuration in the absence of DNA, but swing up and rotate away from the main body of the enzymes when DNA binds (64). During supercoiling, flexibility of the linker region is likely to be important for strand passage but not during relaxation and decatenation. Indeed deletion of the GyrA-CTD converts gyrase into an enzyme that is incapable of catalysing supercoiling but can perform efficient relaxation and decatenation reactions (41).

In relation to the results presented in this article, we propose that Ca^{2+} influences the flexibility or conformation of the linker region. [Proteolysis experiments (Figure 8) support the possibility of Ca^{2+}-mediated conformational changes.] For example, if Ca^{2+} favours the 'down' position of the CTDs then its removal might favour supercoiling over relaxation (Figure 9). It is possible that more complete removal of Ca^{2+}, as in the denaturation/renaturation experiments stabilizes the linker in a conformation that prevents relaxation and decatenation and greatly reduces the flexibility of the linker required for supercoiling. Mutation of the linker amino acids proposed to be involved in Ca^{2+} binding may reduce linker flexibility and/or limit its conformations such that the mobility required for supercoiling is lost because wrapping is greatly disfavoured (Figure 9). Relaxation and decatenation could be largely unaffected under these conditions as the CTDs may be held in a conformation that does not affect these reactions (Figure 9).

An implication from the results in this article is that Ca^{2+} might be involved in the regulation of the activity of gyrase. The role of Ca^{2+} in prokaryotes is less well-established than in eukaryotes, though there is ample evidence for the existence of Ca^{2+}-binding proteins in bacteria (30,46) and a role for Ca^{2+} in a variety of cell processes (e.g. signalling, motility, transport, sporulation, etc.) has been proposed (28). The results presented in this article support the idea that Ca^{2+} may have a regulatory role in *M. tuberculosis* gyrase by modulating the conformation of the linker region between the NTD and the CTD of GyrA as part of a process that favours 'gyrase-like' activities (supercoiling) or 'topo IV-like' activities

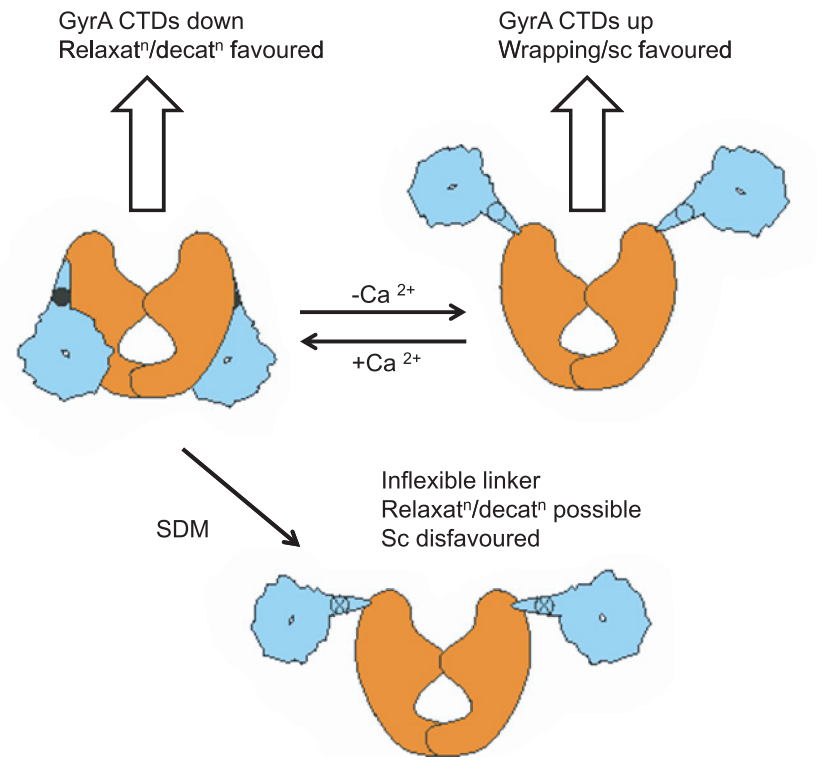

Figure 9. Model for the effect of Ca^{2+}on the conformation of GyrA. GyrA is shown as orange (NTD) and blue (CTD) shapes, based on a previous model for gyrase structure (65); only the GyrA dimer is shown for clarity. The circles in the linker region represent the proposed Ca^{2+}-binding sites: filled circles represent higher Ca^{2+} occupancy than open circles. Site-directed mutagenesis of the binding sites is indicated by the crosses. It is proposed that higher occupancy of the Ca^{2+}-binding sites favours DNA relaxation and decatenation (relaxat^{n}/decat^{n}) by *M. tuberculosis* gyrase and lower occupancy favours supercoiling (sc).

(relaxation/decatenation), i.e. by favouring or disfavouring DNA wrapping. This may be an adaptation for *M. tuberculosis* gyrase (and other gyrases) where there is no topo IV in the bacterium. Verification of this possibility will require further structural work on *M. tuberculosis* GyrA and physiological investigations of the role of Ca^{2+} in *M. tuberculosis*.

SUPPLEMENTARY DATA

Supplementary Data are available at NAR Online: Supplementary Figures 1–5.

ACKNOWLEDGEMENTS

We thank Marcus Edwards and James Taylor for helpful advice, Mike Naldrett, Graham Chilvers and Fiona Husband for scientific support, and James Berger, Fred Collin, V. Nagaraja and Elsa Tretter for their comments on the manuscript.

FUNDING

An EST early stage research scholarship (to S.K.); EU FP7; BBSRC, UK [grant BB/J004561/1]; John Innes Foundation. Funding for open access charge: EU FP7.

Conflict of interest statement. None declared.

REFERENCES

1. Sacchettini,J.C., Rubin,E.J. and Freundlich,J.S. (2008) Drugs versus bugs: in pursuit of the persistent predator Mycobacterium tuberculosis. *Nat. Rev. Microbiol.*, **6**, 41–52.
2. Young,D.B., Perkins,M.D., Duncan,K. and Barry,C.E. III (2008) Confronting the scientific obstacles to global control of tuberculosis. *J. Clin. Invest.*, **118**, 1255–1265.
3. Janin,Y.L. (2007) Antituberculosis drugs: ten years of research. *Bioorg. Med. Chem.*, **15**, 2479–2513.
4. Koul,A., Arnoult,E., Lounis,N., Guillemont,J. and Andries,K. (2011) The challenge of new drug discovery for tuberculosis. *Nature*, **469**, 483–490.
5. Takiff,H. and Guerrero,E. (2011) Current prospects for the fluoroquinolones as first-line tuberculosis therapy. *Antimicrob. Agents Chemother.*, **55**, 5421–5429.
6. Bates,A.D. and Maxwell,A. (2005) *DNA Topology*. Oxford University Press, Oxford.
7. Dong,K.C. and Berger,J.M. (2008) In: Rice,P.A. and Correll,C.C. (eds), *Protein-Nucleic Acid Interactions: Structural Biology*. Royal Society of Chemistry, London.
8. Schoeffler,A.J. and Berger,J.M. (2008) DNA topoisomerases: harnessing and constraining energy to govern chromosome topology. *Q. Rev. Biophys.*, **41**, 41–101.
9. Collin,F., Karkare,S. and Maxwell,A. (2011) Exploiting bacterial DNA gyrase as a drug target: current state and perspectives. *Appl. Microbiol. Biotechnol.*, **92**, 479–497.
10. Pommier,Y., Leo,E., Zhang,H. and Marchand,C. (2010) DNA topoisomerases and their poisoning by anticancer and antibacterial drugs. *Chem. Biol.*, **17**, 421–433.
11. Tse-Dinh,Y.C. (2007) Exploring DNA topoisomerases as targets of novel therapeutic agents in the treatment of infectious diseases. *Infect. Disord. Drug. Targets*, **7**, 3–9.
12. Nollmann,M., Crisona,N.J. and Arimondo,P.B. (2007) Thirty years of Escherichia coli DNA gyrase: from in vivo function to single-molecule mechanism. *Biochimie*, **89**, 490–499.

13. Reece,R.J. and Maxwell,A. (1991) DNA gyrase: structure and function. *CRC Crit. Rev. Biochem. Mol. Biol.*, **26**, 335–375.
14. Zechiedrich,E.L. and Cozzarelli,N.R. (1995) Roles of topoisomerase IV and DNA gyrase in DNA unlinking during replication in Escherichia coli. *Genes Dev.*, **9**, 2859–2869.
15. Zechiedrich,E.L., Khodursky,A.B., Bachellier,S., Schneider,R., Chen,D., Lilley,D.M.J. and Cozzarelli,N.R. (2000) Roles of topoisomerases in maintaining steady-state DNA supercoiling in *Escherichia coli*. *J. Biol. Chem.*, **275**, 8103–8113.
16. Levine,C., Hiasa,H. and Marians,K.J. (1998) DNA gyrase and topoisomerase IV: biochemical activities, physiological roles during chromosome replication, and drug sensitivities. *Biochim. Biophys. Acta*, **1400**, 29–43.
17. Aubry,A., Pan,X.S., Fisher,L.M., Jarlier,V. and Cambau,E. (2004) Mycobacterium tuberculosis DNA gyrase: interaction with quinolones and correlation with antimycobacterial drug activity. *Antimicrob. Agents Chemother.*, **48**, 1281–1288.
18. Cole,S.T., Brosch,R., Parkhill,J., Garnier,T., Churcher,C., Harris,D., Gordon,S.V., Eiglmeier,K., Gas,S., Barry,C.E. III *et al.* (1998) Deciphering the biology of Mycobacterium tuberculosis from the complete genome sequence. *Nature*, **393**, 537–544.
19. Jain,P. and Nagaraja,V. (2005) An atypical type II topoisomerase from Mycobacterium smegmatis with positive supercoiling activity. *Mol. Microbiol.*, **58**, 1392–1405.
20. Aubry,A., Fisher,L.M., Jarlier,V. and Cambau,E. (2006) First functional characterization of a singly expressed bacterial type II topoisomerase: the enzyme from Mycobacterium tuberculosis. *Biochem. Biophys. Res. Commun.*, **348**, 158–165.
21. Manjunatha,U.H., Dalal,M., Chatterji,M., Radha,D.R., Visweswariah,S.S. and Nagaraja,V. (2002) Functional characterisation of mycobacterial DNA gyrase: an efficient decatenase. *Nucleic Acids Res.*, **30**, 2144–2153.
22. Huang,Y.Y., Deng,J.Y., Gu,J., Zhang,Z.P., Maxwell,A., Bi,L.J., Chen,Y.Y., Zhou,Y.F., Yu,Z.N. and Zhang,X.E. (2006) The key DNA-binding residues in the C-terminal domain of Mycobacterium tuberculosis DNA gyrase A subunit (GyrA). *Nucleic Acids Res.*, **34**, 5650–5659.
23. Wu,J., Zhang,Z., Mitchenall,L.A., Maxwell,A., Deng,J., Zhang,H., Zhou,Y., Chen,Y.Y., Wang,D.C., Zhang,X.E. *et al.* (2011) The dimer state of GyrB is an active form: implications for the initial complex assembly and processive strand passage. *Nucleic Acids Res.*, **39**, 8488–8502.
24. Fu,G., Wu,J., Liu,W., Zhu,D., Hu,Y., Deng,J., Zhang,X.E., Bi,L. and Wang,D.C. (2009) Crystal structure of DNA gyrase B' domain sheds lights on the mechanism for T-segment navigation. *Nucleic Acids Res.*, **37**, 5908–5916.
25. Piton,J., Petrella,S., Delarue,M., Andre-Leroux,G., Jarlier,V., Aubry,A. and Mayer,C. (2010) Structural insights into the quinolone resistance mechanism of Mycobacterium tuberculosis DNA gyrase. *PLoS ONE*, **5**, e12245.
26. Tretter,E.M., Schoeffler,A.J., Weisfield,S.R. and Berger,J.M. (2010) Crystal structure of the DNA gyrase GyrA N-terminal domain from Mycobacterium tuberculosis. *Proteins*, **78**, 492–495.
27. Tretter,E.M. and Berger,J.M. (2012) Mechanisms for defining supercoiling set point of DNA gyrase orthologs: II. The shape of the GyrA subunit C-terminal domain (CTD) is not a sole determinant for controlling supercoiling efficiency. *J. Biol. Chem.*, **287**, 18645–18654.
28. Dominguez,D.C. (2004) Calcium signalling in bacteria. *Mol. Microbiol.*, **54**, 291–297.
29. Holland,I.B., Jones,H.E., Campbell,A.K. and Jacq,A. (1999) An assessment of the role of intracellular free Ca2+ in *E. coli*. *Biochimie*, **81**, 901–907.
30. Michiels,J., Xi,C., Verhaert,J. and Vanderleyden,J. (2002) The functions of Ca(2+) in bacteria: a role for EF-hand proteins? *Trends Microbiol.*, **10**, 87–93.
31. Larkin,M.A., Blackshields,G., Brown,N.P., Chenna,R., McGettigan,P.A., McWilliam,H., Valentin,F., Wallace,I.M., Wilm,A., Lopez,R. *et al.* (2007) Clustal W and Clustal X version 2.0. *Bioinformatics*, **23**, 2947–2948.
32. Edgar,R.C. (2004) MUSCLE: a multiple sequence alignment method with reduced time and space complexity. *BMC Bioinformatics*, **5**, 113.
33. Edgar,R.C. (2004) MUSCLE: multiple sequence alignment with high accuracy and high throughput. *Nucleic Acids Res.*, **32**, 1792–1797.
34. Jones,D.T. (1999) Protein secondary structure prediction based on position-specific scoring matrices. *J. Mol. Biol.*, **292**, 195–202.
35. Gasteiger,E., Gattiker,A., Hoogland,C., Ivanyi,I., Appel,R.D. and Bairoch,A. (2003) ExPASy: The proteomics server for in-depth protein knowledge and analysis. *Nucleic Acids Res.*, **31**, 3784–3788.
36. Kelley,L.A. and Sternberg,M.J. (2009) Protein structure prediction on the Web: a case study using the Phyre server. *Nat. Protoc.*, **4**, 363–371.
37. Ginalski,K., Elofsson,A., Fischer,D. and Rychlewski,L. (2003) 3D-Jury: a simple approach to improve protein structure predictions. *Bioinformatics*, **19**, 1015–1018.
38. Hockings,S.C. and Maxwell,A. (2002) Identification of four GyrA residues involved in the DNA breakage-reunion reaction of DNA gyrase. *J. Mol. Biol.*, **318**, 351–359.
39. Reece,R.J. and Maxwell,A. (1989) Tryptic fragments of the *Escherichia coli* DNA gyrase A protein. *J. Biol. Chem.*, **264**, 19648–19653.
40. Reece,R.J. and Maxwell,A. (1991) Probing the limits of the DNA breakage-reunion domain of the *Escherichia coli* DNA gyrase A protein. *J. Biol. Chem.*, **266**, 3540–3546.
41. Kampranis,S.C. and Maxwell,A. (1996) Conversion of DNA gyrase into a conventional type II topoisomerase. *Proc. Natl Acad. Sci. USA*, **93**, 14416–14421.
42. Reece,R.J. and Maxwell,A. (1991) The C-terminal domain of the *Escherichia coli* DNA gyrase A subunit is a DNA-binding protein. *Nucleic Acids Res.*, **19**, 1399–1405.
43. Baker,N.M., Weigand,S., Maar-Mathias,S. and Mondragon,A. (2011) Solution structures of DNA-bound gyrase. *Nucleic Acids Res.*, **39**, 755–766.
44. Costenaro,L., Grossmann,J.G., Ebel,C. and Maxwell,A. (2005) Small-angle X-ray scattering reveals the solution structure of the full-length DNA gyrase A subunit. *Structure*, **13**, 287–296.
45. Corbett,K.D., Schoeffler,A.J., Thomsen,N.D. and Berger,J.M. (2005) The structural basis for substrate specificity in DNA topoisomerase IV. *J. Mol. Biol.*, **351**, 545–561.
46. Zhou,Y., Yang,W., Kirberger,M., Lee,H.W., Ayalasomayajula,G. and Yang,J.J. (2006) Prediction of EF-hand calcium-binding proteins and analysis of bacterial EF-hand proteins. *Proteins*, **65**, 643–655.
47. Gifford,J.L., Walsh,M.P. and Vogel,H.J. (2007) Structures and metal-ion-binding properties of the Ca2+-binding helix-loop-helix EF-hand motifs. *Biochem. J.*, **405**, 199–221.
48. Grabarek,Z. (2006) Structural basis for diversity of the EF-hand calcium-binding proteins. *J. Mol. Biol.*, **359**, 509–525.
49. Kawasaki,H., Nakayama,S. and Kretsinger,R.H. (1998) Classification and evolution of EF-hand proteins. *Biometals*, **11**, 277–295.
50. Ravasi,T., Hsu,K., Goyette,J., Schroder,K., Yang,Z., Rahimi,F., Miranda,L.P., Alewood,P.F., Hume,D.A. and Geczy,C. (2004) Probing the S100 protein family through genomic and functional analysis. *Genomics*, **84**, 10–22.
51. Vyas,N.K., Vyas,M.N. and Quiocho,F.A. (1987) A novel calcium binding site in the galactose-binding protein of bacterial transport and chemotaxis. *Nature*, **327**, 635–638.
52. Mishima,Y., Momma,K., Hashimoto,W., Mikami,B. and Murata,K. (2003) Crystal structure of AlgQ2, a macromolecule (alginate)-binding protein of Sphingomonas sp. A1, complexed with an alginate tetrasaccharide at 1.6-A resolution. *J. Biol. Chem.*, **278**, 6552–6559.
53. Aghajari,N., Van Petegem,F., Villeret,V., Chessa,J.P., Gerday,C., Haser,R. and Van Beeumen,J. (2003) Crystal structures of a psychrophilic metalloprotease reveal new insights into catalysis by cold-adapted proteases. *Proteins*, **50**, 636–647.
54. Banbula,A., Potempa,J., Travis,J., Fernandez-Catalan,C., Mann,K., Huber,R., Bode,W. and Medrano,F. (1998) Amino-acid sequence and three-dimensional structure of the Staphylococcus aureus metalloproteinase at 1.72 A resolution. *Structure*, **6**, 1185–1193.

55. Noble,C.G. and Maxwell,A. (2002) The role of GyrB in the DNA cleavage-religation reaction of DNA gyrase: a proposed two-metal-ion mechanism. *J. Mol. Biol.*, **318**, 361–371.
56. Kampranis,S.C., Bates,A.D. and Maxwell,A. (1999) A model for the mechanism of strand passage by DNA gyrase. *Proc. Natl Acad. Sci. USA*, **96**, 8414–8419.
57. Frothingham,R. (1995) Differentiation of strains in Mycobacterium tuberculosis complex by DNA sequence polymorphisms, including rapid identification of *M. bovis BCG*. *J. Clin. Microbiol.*, **33**, 840–844.
58. Schmutz,E., Hennig,S., Li,S.M. and Heide,L. (2004) Identification of a topoisomerase IV in actinobacteria: purification and characterization of ParY(R) and GyrB(R) from the coumermycin A(1) producer *Streptomyces rishiriensis* DSM 40489. *Microbiology*, **150**, 641–647.
59. Sierra,J.M., Martinez-Martinez,L., Vazquez,F., Giralt,E. and Vila,J. (2005) Relationship between mutations in the gyrA gene and quinolone resistance in clinical isolates of Corynebacterium striatum and Corynebacterium amycolatum. *Antimicrob. Agents Chemother.*, **49**, 1714–1719.
60. Waltersson,Y., Linse,S., Brodin,P. and Grundstrom,T. (1993) Mutational effects on the cooperativity of Ca2+ binding in calmodulin. *Biochemistry*, **32**, 7866–7871.
61. Black,D.J., Tikunova,S.B., Johnson,J.D. and Davis,J.P. (2000) Acid pairs increase the N-terminal Ca2+ affinity of CaM by increasing the rate of Ca2+ association. *Biochemistry*, **39**, 13831–13837.
62. Heddle,J.G., Mitelheiser,S., Maxwell,A. and Thomson,N.H. (2004) Nucleotide binding to DNA gyrase causes loss of DNA wrap. *J. Mol. Biol.*, **337**, 597–610.
63. Kirchhausen,T., Wang,J.C. and Harrison,S.C. (1985) DNA gyrase and its complexes with DNA: direct observation by electron microscopy. *Cell*, **41**, 933–943.
64. Lanz,M.A. and Klostermeier,D. (2011) Guiding strand passage: DNA-induced movement of the gyrase C-terminal domains defines an early step in the supercoiling cycle. *Nucleic Acids Res.*, **39**, 9681–9694.
65. Costenaro,L., Grossmann,J.G., Ebel,C. and Maxwell,A. (2007) Modular structure of the full-length DNA gyrase B subunit revealed by small-angle X-ray scattering. *Structure*, **15**, 329–339.